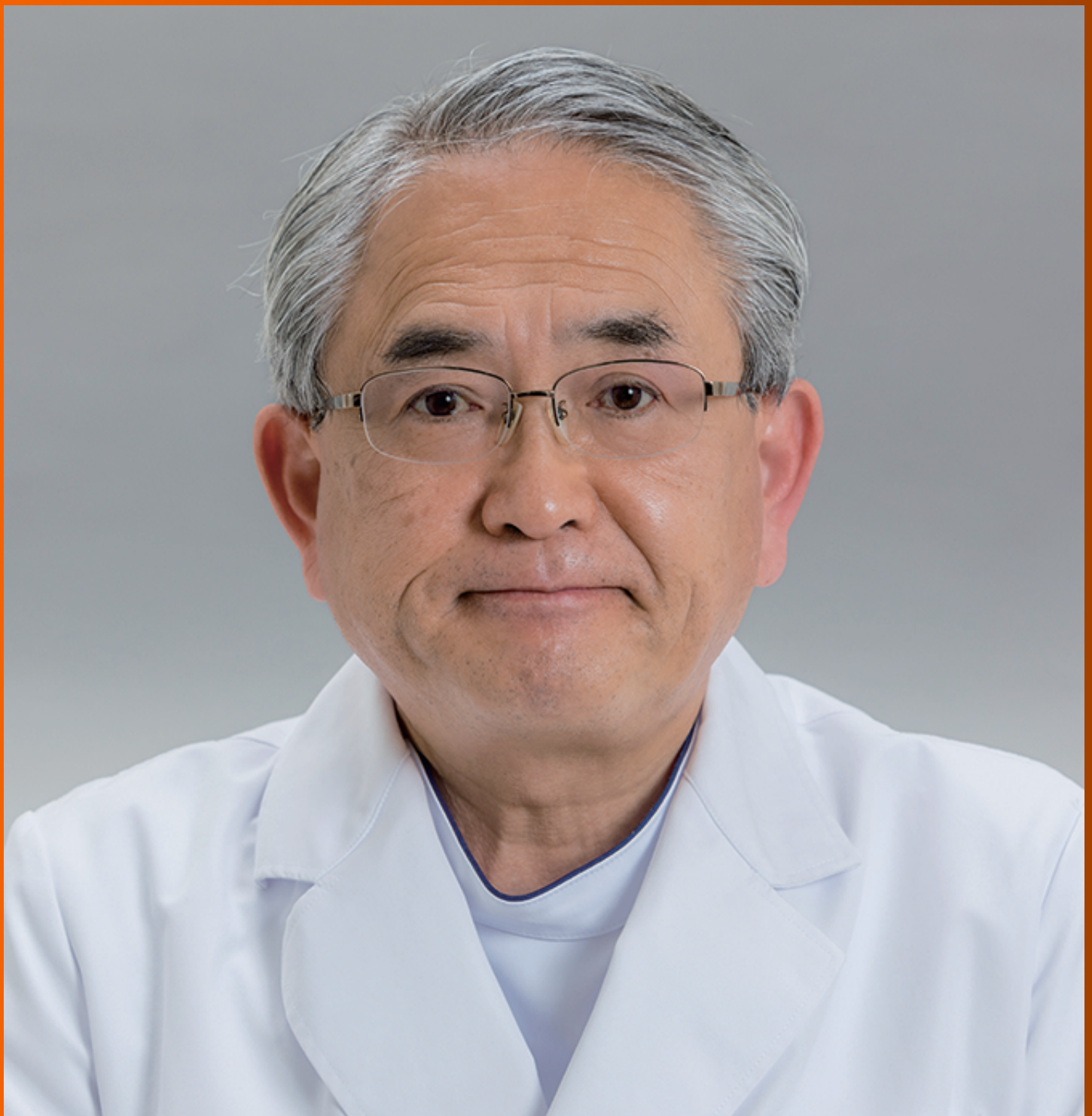


# World Journal of *Gastroenterology*

*World J Gastroenterol* 2024 July 7; 30(25): 3126-3184



**EDITORIAL**

- 3126 Large non-pedunculated colorectal polyp management: The elephant in the room  
*Jiang SX, Shahidi N*
- 3132 Alanine aminotransferase as a risk marker for new-onset metabolic dysfunction-associated fatty liver disease  
*Wang D, Zhou BY, Xiang L, Chen XY, Feng JX*
- 3140 Refining the targeted population and achieving better for colorectal cancer screening  
*Zhou NY, Lin YX, Chen LX, Ye LS, Hu B*
- 3143 Quantitative assessment of self-management in patients with non-alcoholic fatty liver disease: An unmet clinical need  
*Borriello R, Esposito G, Mignini I, Gasbarrini A, Zocco MA*
- 3147 Risk of hepatic decompensation from hepatitis B virus reactivation in hematological malignancy treatments  
*Barone M*
- 3152 Double-nylon purse-string suture technique: Another addition to the endoscopist's toolbox for full-thickness defect closure  
*Walia A, Trasolini RP, Shahidi N*

**ORIGINAL ARTICLE****Retrospective Study**

- 3155 Computed tomography-based radiomics combined with machine learning allows differentiation between primary intestinal lymphoma and Crohn's disease  
*Xiao MJ, Pan YT, Tan JH, Li HO, Wang HY*
- 3166 Predicting hepatocellular carcinoma: A new non-invasive model based on shear wave elastography  
*Jiang D, Qian Y, Gu YJ, Wang R, Yu H, Dong H, Chen DY, Chen Y, Jiang HZ, Tan BB, Peng M, Li YR*

**LETTER TO THE EDITOR**

- 3179 Scale offers the possibility of identifying adherence to lifestyle interventions in patients with non-alcoholic fatty liver disease  
*Liu CQ, Hu B*
- 3182 Back to the drawing board: Overview of the next generation of combination therapy for inflammatory bowel disease  
*Lowell JA, Farber MJ, Sultan K*

**ABOUT COVER**

Editorial Board Member of *World Journal of Gastroenterology*, Kentaro Yoshioka, MD, PhD, Director, Center for Liver Diseases, Meijo Hospital, Nagoya 460-0001, Aichi, Japan. kyoshiok8@gmail.com

**AIMS AND SCOPE**

The primary aim of *World Journal of Gastroenterology* (WJG, *World J Gastroenterol*) is to provide scholars and readers from various fields of gastroenterology and hepatology with a platform to publish high-quality basic and clinical research articles and communicate their research findings online. WJG mainly publishes articles reporting research results and findings obtained in the field of gastroenterology and hepatology and covering a wide range of topics including gastroenterology, hepatology, gastrointestinal endoscopy, gastrointestinal surgery, gastrointestinal oncology, and pediatric gastroenterology.

**INDEXING/ABSTRACTING**

The WJG is now abstracted and indexed in Science Citation Index Expanded (SCIE), MEDLINE, PubMed, PubMed Central, Scopus, Reference Citation Analysis, China Science and Technology Journal Database, and Superstar Journals Database. The 2024 edition of Journal Citation Reports® cites the 2023 journal impact factor (JIF) for WJG as 4.3; Quartile: Q1. The WJG's CiteScore for 2023 is 7.8.

**RESPONSIBLE EDITORS FOR THIS ISSUE**

Production Editor: *Hua-Ge Yu*; Production Department Director: *Xu Guo*; Cover Editor: *Jia-Ru Fan*.

**NAME OF JOURNAL**

*World Journal of Gastroenterology*

**ISSN**

ISSN 1007-9327 (print) ISSN 2219-2840 (online)

**LAUNCH DATE**

October 1, 1995

**FREQUENCY**

Weekly

**EDITORS-IN-CHIEF**

Andrzej S Tarnawski

**EXECUTIVE ASSOCIATE EDITORS-IN-CHIEF**

Xian-Jun Yu (Pancreatic Oncology), Jian-Gao Fan (Chronic Liver Disease), Hou-Bao Liu

**EDITORIAL BOARD MEMBERS**

<http://www.wjgnet.com/1007-9327/editorialboard.htm>

**PUBLICATION DATE**

July 7, 2024

**COPYRIGHT**

© 2024 Baishideng Publishing Group Inc

**PUBLISHING PARTNER**

Shanghai Pancreatic Cancer Institute and Pancreatic Cancer Institute, Fudan University  
Biliary Tract Disease Institute, Fudan University

**INSTRUCTIONS TO AUTHORS**

<https://www.wjgnet.com/bpg/gcrinfo/204>

**GUIDELINES FOR ETHICS DOCUMENTS**

<https://www.wjgnet.com/bpg/GerInfo/287>

**GUIDELINES FOR NON-NATIVE SPEAKERS OF ENGLISH**

<https://www.wjgnet.com/bpg/gcrinfo/240>

**PUBLICATION ETHICS**

<https://www.wjgnet.com/bpg/GerInfo/288>

**PUBLICATION MISCONDUCT**

<https://www.wjgnet.com/bpg/gcrinfo/208>

**POLICY OF CO-AUTHORS**

<https://www.wjgnet.com/bpg/GerInfo/310>

**ARTICLE PROCESSING CHARGE**

<https://www.wjgnet.com/bpg/gcrinfo/242>

**STEPS FOR SUBMITTING MANUSCRIPTS**

<https://www.wjgnet.com/bpg/GerInfo/239>

**ONLINE SUBMISSION**

<https://www.f6publishing.com>

**PUBLISHING PARTNER'S OFFICIAL WEBSITE**

<https://www.shca.org.cn>  
<https://www.zs-hospital.sh.cn>

## Retrospective Study

# Computed tomography-based radiomics combined with machine learning allows differentiation between primary intestinal lymphoma and Crohn's disease

Meng-Jun Xiao, Yu-Teng Pan, Jia-He Tan, Hai-Ou Li, Hai-Yan Wang

**Specialty type:** Radiology, nuclear medicine and medical imaging**Provenance and peer review:** Unsolicited article; Externally peer reviewed.**Peer-review model:** Single blind**Peer-review report's classification****Scientific Quality:** Grade B**Novelty:** Grade B**Creativity or Innovation:** Grade B**Scientific Significance:** Grade B**P-Reviewer:** Mohey NM, Egypt**Received:** January 9, 2024**Revised:** May 20, 2024**Accepted:** June 7, 2024**Published online:** July 7, 2024**Processing time:** 174 Days and 3.6 Hours**Meng-Jun Xiao, Hai-Yan Wang**, Department of Radiology, Shandong Provincial Hospital Affiliated to Shandong First Medical University, Jinan 250021, Shandong Province, China**Yu-Teng Pan**, Medical Science and Technology Innovation Center, Shandong First Medical University & Shandong Academy of Medical Sciences, Jinan 250000, Shandong Province, China**Jia-He Tan**, University of California, Davis, CA 95616, United States**Hai-Ou Li**, Qilu Hospital, Cheeloo College of Medicine, Shandong University, Jinan 250012, Shandong Province, China**Co-first authors:** Meng-Jun Xiao and Yu-Teng Pan.**Corresponding author:** Hai-Yan Wang, MD, PhD, Professor, Department of Radiology, Shandong Provincial Hospital Affiliated to Shandong First Medical University, No. 324 Jingwu Road, Jinan 250021, Shandong Province, China. [whyott@163.com](mailto:whyott@163.com)

## Abstract

### BACKGROUND

Due to similar clinical manifestations and imaging signs, differential diagnosis of primary intestinal lymphoma (PIL) and Crohn's disease (CD) is a challenge in clinical practice.

### AIM

To investigate the ability of radiomics combined with machine learning methods to differentiate PIL from CD.

### METHODS

We collected contrast-enhanced computed tomography (CECT) and clinical data from 120 patients from center 1. A total of 944 features were extracted single-phase images of CECT scans. Using the last absolute shrinkage and selection operator model, the best predictive radiographic features and clinical indications were screened. Data from 54 patients were collected at center 2 as an external validation set to verify the robustness of the model. The area under the receiver operating characteristic curve, accuracy, sensitivity and specificity were used for

evaluation.

## RESULTS

A total of five machine learning models were built to distinguish PIL from CD. Based on the results from the test group, most models performed well with a large area under the curve (AUC) (> 0.850) and high accuracy (> 0.900). The combined clinical and radiomics model (AUC = 1.000, accuracy = 1.000) was the best model among all models.

## CONCLUSION

Based on machine learning, a model combining clinical data with radiologic features was constructed that can effectively differentiate PIL from CD.

**Key Words:** Primary intestinal lymphoma; Crohn's disease; Radiomics; Machine learning; Diagnosis

©The Author(s) 2024. Published by Baishideng Publishing Group Inc. All rights reserved.

**Core Tip:** In the present study employed radiomics to extract features from computed tomography images of primary intestinal lymphoma and Crohn's disease, followed by the construction of machine learning models for improved differentiation between these two conditions. The least absolute shrinkage and selection operator regression model with 5-fold cross validation was utilized for feature selection, resulting in the identification of 13 optimal predictive radiomics features along with 4 clinical features. Ultimately, all phase models incorporating radiomics features and a combined model integrating both radiomics and clinical features were developed.

**Citation:** Xiao MJ, Pan YT, Tan JH, Li HO, Wang HY. Computed tomography-based radiomics combined with machine learning allows differentiation between primary intestinal lymphoma and Crohn's disease. *World J Gastroenterol* 2024; 30(25): 3155-3165

**URL:** <https://www.wjgnet.com/1007-9327/full/v30/i25/3155.htm>

**DOI:** <https://dx.doi.org/10.3748/wjg.v30.i25.3155>

## INTRODUCTION

Intestinal lymphoma is the second most common extralymph node lymphoma after gastric lymphoma and is occurring with a general uptrend in incidence worldwide[1,2]. The National Cancer Institute's Surveillance, Epidemiology, and End Results database showed that the incidence of lymphoma in the small intestine and colon increased from 0.22 and 0.1 in 1973 to 0.35 and 0.21 in 2004, respectively[3]. Among these lymphomas, primary intestinal lymphoma (PIL) is very rare, accounting for only approximately 15% of intestinal malignancies[4,5], but lacks specific clinical manifestations. Abdominal pain is the most common clinical symptom, followed by abdominal mass, nausea, anorexia, gastrointestinal bleeding, intestinal obstruction, *etc*[6-8]. Crohn's disease (CD) is a chronic inflammatory granulomatous disease of the gastrointestinal tract that develops in a recurrent and remitting manner and is influenced by genetic, immune and environmental influences, with increasing incidence worldwide[9-11]. Both PIL and CD can present with clinical symptoms similar to other intestinal diseases, but both diseases can be distinguished from other intestinal diseases by imaging and pathology. However, the diagnosis of PIL and CD can be easily confused because they are not only similar in clinical presentation, but also have many overlapping imaging and endoscopic features[2,7,12]. It is worth noting that PIL and CD differ greatly in terms of clinical treatments as CD is often treated with drugs such as aminosalicylic acid, whereas PIL can be treated with observation, chemotherapy, or a combination of chemotherapy and surgery depending on the type of pathology[6,8,10,13]. Therefore, distinguishing PIL from CD remains a radiographic diagnostic challenge.

Contrast-enhanced computed imaging plays an important role in the diagnosis of CD and intestinal lymphoma and allows for evaluation of areas of the gastrointestinal tract that are not accessible by conventional upper gastrointestinal endoscopy and colonoscopy[2,13,14]. In some previous studies, various features have been applied as diagnostic points in PIL and CD, including demographic, clinical, endoscopic, endoscopy and computed tomography enterography data[7]. However, sometimes it is difficult to distinguish PIL from CD due to similar imaging manifestations in real-time clinical work.

Radiomics is a rapidly growing field built on computer-aided diagnostic, prognostic, and therapeutic research, involving specifically the high-throughput extraction of quantitative features from radiographic images, the conversion of images into mineable data and, thus, risk assessment by incorporating imaging features into predictive models of treatment outcomes[15-18]. Machine learning lies at the intersection of computer science and statistics and is a scientific discipline that encompasses the study of how computers learn from data. It arises at the intersection of statistics, which seeks to learn relationships from data, and computer science, which emphasizes efficient computational algorithms[19, 20]. Liu *et al*[4] performed texture analysis of arteriovenous computed tomography (CT) images of patients to differentiate small intestinal lymphomas from nonlymphomas. Zhang *et al*[7] identified CD and PIL by evaluating different parameters. However, very little attention has been given to the diagnostic imaging of PIL and CD in terms of radiomics combined with machine learning. In this study, we performed the extraction of multiple radiomic features to combine

statistically significant clinical indications with histological features to build a higher performance classification model.

Therefore, the main objective of this study was to develop a multiphase enhanced CT-based radiomics combined with machine learning model to discriminate PIL from CD by detecting subtle changes and, thereby, help to guide the choice of clinical treatment modality.

## MATERIALS AND METHODS

### Patients

This was a retrospective study approved by the institutional review board of the Ethics Committee. Informed consent was waived because of the retrospective nature of the study. We reviewed the medical records of 264 patients diagnosed with PIL and CD between January 2011 and January 2023 at Shandong First Medical University Affiliated Provincial Hospital. Finally, 120 patients (69 PIL patients with histologically confirmed and 51 CD patients with a clinical diagnosis including biopsy pathology) who met the inclusion criteria were included in this study (center 1). We collected 54 patients from Qilu Hospital of Shandong University between June 2015 to August 2022 (center 2). The requirement for informed consent was waived due to the retrospective nature of this study. Flowchart of participant selection is detailed in [Supplementary Figure 1](#).

Patients with PIL were included according to the Dawson criteria[21]. Patients with CD were included according to the following criteria: (1) Clinician diagnosis of CD; (2) Pathology and CT examination performed during hospitalization; and (3) No previous intestinal surgical treatment. All above patients were excluded according to the following criteria: (1) Patients with both PIL and CD; (2) Patients with other concomitant gastrointestinal diseases; and (3) Lack of clinical data or CT images. The basic clinical data were recorded and displayed. The non-contrast enhanced phase, arterial phase and venous phase CT images of all patients were collected.

### CT imaging and the region of interest

The CT scan protocols are shown in [Supplementary Table 1](#). The nonionic contrast medium (iopromide, ultravist 370; Bayer) was administered into the antecubital vein by a power injector at a rate of 2.5 mL/s. Non contrast CT of the whole abdomen was performed first, followed by two postcontrast CT scans obtained in the arterial phase and venous phase. Based on the non-contrast-enhanced phase, arterial phase and venous phase CT images, the region of interest (ROI) were depicted manually and individually by an abdominal radiologist with 3 years of experience using ITK-SNAP open source software version 3.6.0 (Yushkevich P and Gerig G) without knowledge of the patient's clinical data, the images were examined by an abdominal radiologist with 26 years of experience, and the outlined area did not include the intestinal cavity and blood vessels[22].

### Feature extraction

The CT images were normalized by performing a rescaling operation. The slice thickness was standardized by resampled voxel sizes to 1 mm × 1 mm × 5 mm. The features of ROIs were extracted by using the pyradiomics package version 3.0.1. A total of 944 radiomics features were extracted from every single-phase CT images of each patient, including 14 shape features, 180 first-order features and 750 texture features. The texture features were calculated by using Gray Level Cooccurrence Matrix, Gray Level Dependence Matrix, Gray Level Run Length Matrix, Gray Level Size Zone Matrix and Neighborhood Gray-tone Difference Matrix.

### Feature selection

A total of 120 patients from center 1 were randomly divided into a training set ( $n = 84$ ) and an internal validation set ( $n = 36$ ) at a 7:3 ratio. The least absolute shrinkage and selection operator (Lasso) can select variables while estimating model parameters and better solve the multicollinearity problem in regression analysis. Based on the training set, the best predictive radiomics features were selected by using the Lasso model with 5-fold cross validation to reduce overfitting. In addition, lasso model with 5-fold cross validation was also used to select statistically significant clinical features. The median value and  $p$ -value of selected radiomics feature is presented in [Table 1](#).

### Model establishment and assessment

Five machine learning models were established to classify CD and PIL. First, three lasso models were established by radiomics features selected based on the non-contrast enhanced phase, arterial phase and venous phase single-phase CT images respectively. Next, two logistic regression models were established including an all phase model and a combined (clinical and radiomics) model. The establishment of all phase model was based on the features selected by three single-phase selections. The establishment of the combined model was based on the three single-phase radiomics and clinical features.

The models were assessed by the area under the curve (AUC) of receive operating curve, accuracy, sensitivity and specificity. Then, the calibration curve was used to assess the conformity between the predicted and actual results. The patients from center 2 acted as an external validation set to demonstrate the robustness of the models. The flowchart of model construction was presented in [Figure 1](#).

### Statistical analysis

ITK-SNAP version 3.6.0 is an open-source software (<http://www.itksnap.org/pmwiki/pmwiki.php>)[22]. Statistical

**Table 1** The median value of selected radiomics feature

Datasets		Training set			Internal validation set			External validation set		
		CD	PIL	P value	CD	PIL	P value	CD	PIL	P value
Phases	Features									
N	OSV	0.58	0.38	0.00 <sup>b</sup>	0.63	0.36	0.00 <sup>b</sup>	0.60	0.39	0.00 <sup>b</sup>
	LSGL	-0.19	-0.28	0.00 <sup>b</sup>	-0.23	-0.28	0.11	-0.25	-0.30	0.10
	WLLHGR	0.81	0.68	0.00 <sup>b</sup>	0.83	0.70	0.00 <sup>b</sup>	0.70	0.61	0.09
	WHLLFM	-2.61	-0.60	0.00 <sup>b</sup>	-2.99	-0.64	0.00 <sup>b</sup>	-1.52	-0.86	0.01 <sup>a</sup>
	WHHHGL	2.35	3.21	0.00 <sup>b</sup>	2.21	2.89	0.00 <sup>b</sup>	2.65	3.28	0.00 <sup>b</sup>
A	OSV	0.58	0.37	0.00 <sup>b</sup>	0.62	0.39	0.00 <sup>b</sup>	0.62	0.40	0.00 <sup>b</sup>
	WHLLFM	-2.96	-0.65	0.00 <sup>b</sup>	-4.42	-0.85	0.00 <sup>b</sup>	-1.77	-0.80	0.00 <sup>b</sup>
	WLLLGR	0.84	0.73	0.00 <sup>b</sup>	0.85	0.72	0.00 <sup>b</sup>	0.77	0.69	0.00 <sup>b</sup>
V	OSV	0.55	0.37	0.00 <sup>b</sup>	0.70	0.37	0.00 <sup>b</sup>	0.59	0.40	0.00 <sup>b</sup>
	LSGL	-0.18	-0.28	0.00 <sup>b</sup>	-0.20	-0.25	0.03 <sup>a</sup>	-0.23	-0.30	0.00 <sup>b</sup>
	WHLLFM	-2.90	-0.77	0.00 <sup>b</sup>	-5.08	-0.68	0.00 <sup>b</sup>	-1.93	-1.05	0.00 <sup>b</sup>
	WLLLGA	0.17	0.10	0.00 <sup>b</sup>	0.18	0.10	0.00 <sup>b</sup>	0.14	0.08	0.00 <sup>b</sup>
	WLLLGR	0.84	0.74	0.00 <sup>b</sup>	0.85	0.71	0.00 <sup>b</sup>	0.79	0.69	0.00 <sup>b</sup>

<sup>a</sup>*P* < 0.05.

<sup>b</sup>*P* < 0.01.

PIL: Primary intestinal lymphoma; CD: Crohn's disease; N: Non-contrast enhanced; A: Arterial; V: Venous; OSV: Original shape voxel volume; LSGL: Log sigma 3-0-mm-3D glcm lmc2; WLLHGR: Wavelet LLH glrlm run percentage; WHLLFM: Wavelet HLL firstorder minimum; WHHHGL: Wavelet HHH glrlm long run high gray level emphasis; WLLLGR: Wavelet LLL glrlm run percentage; WLLLGA: Wavelet LLL glcm autocorrelation.

analyses were performed using R Version 3.4.0 (<https://www.r-project.org/>).

## RESULTS

### Patients

A total of 120 patients (51 CD and 69 PIL) from center 1 and 54 patients (30 CD and 24 PIL) from center 2 were enrolled in this study. The clinical characteristics were shown in [Supplementary Table 2](#).

### Feature selection and the establishment and assessment of model

After selection with lasso regression, the non-contrast enhanced phase, arterial phase and venous phase models were built with five, three and five optimal radiomics features, respectively. All phase model was built by the above thirteen radiomics features. After selection with Lasso, four clinical features were selected including frequency of defecation, intestinal wall thickness, comb sign and enhanced pattern. Finally, the above thirteen radiomics features and four clinical features were combined to build the radiomics and clinical combined model, and the nomogram was created ([Figure 2](#)).

The AUC of non-contrast enhanced phase, arterial phase and venous phase in the training set, internal validation set and external validation set was as follows: 0.942, 0.867 and 0.858; 0.939, 0.905 and 0.850; 0.943, 0.898 and 0.860. The AUC of all phase model was 0.987, 0.959 and 0.975 in the training set, internal validation set and external validation set, respectively. The AUC of the combined model was 1.000, 0.987 and 1.000 in the training set, internal validation set and external validation set, respectively ([Figure 3](#)). The accuracy, specificity and sensitivity of all models are shown in [Table 2](#). The confusion matrix and calibration curve show that the models have good classification ability ([Figures 4 and 5](#)).

## DISCUSSION

PIL and CD share many similarities in clinical symptoms and imaging features, including manifestations of abdominal pain, hematochezia, thickening of the intestinal wall and abnormal enhancement. In addition, the clinical treatment modalities of PIL and CD are completely different, and delayed diagnosis may lead to complications. Therefore, the rapid diagnosis and differentiation of PIL and CD is an urgent need for clinicians and has important guiding significance for the choice of treatment methods.

**Table 2** The performance of models in the internal/external validation set

Dataset	Score	Radiomics (All phase)	Combined (radiomics + clinical)
Internal validation set	AUC	0.96 (95%CI: 0.90-1.00)	0.99 (95%CI: 0.96-1.00)
	Accuracy	0.92 (95%CI: 0.78-0.98)	0.94 (95%CI: 0.81-1.00)
	Sensitivity	0.93 (95%CI: 0.68-1.00)	1.00 (95%CI: 0.78-1.00)
	Specificity	0.91 (95%CI: 0.70-1.00)	0.91 (95%CI: 0.70-1.00)
External validation set	AUC	0.98 (95%CI: 0.94-1.00)	1.00 (95%CI: 0.99-1.00)
	Accuracy	0.93 (95%CI: 0.82-0.98)	1.00 (95%CI: 0.93-1.00)
	Sensitivity	0.96 (95%CI: 0.79-1.00)	1.00 (95%CI: 0.86-1.00)
	Specificity	0.90 (95%CI: 0.73-0.98)	1.00 (95%CI: 0.88-1.00)

AUC: Area under the curve; CI: Confidence interval.

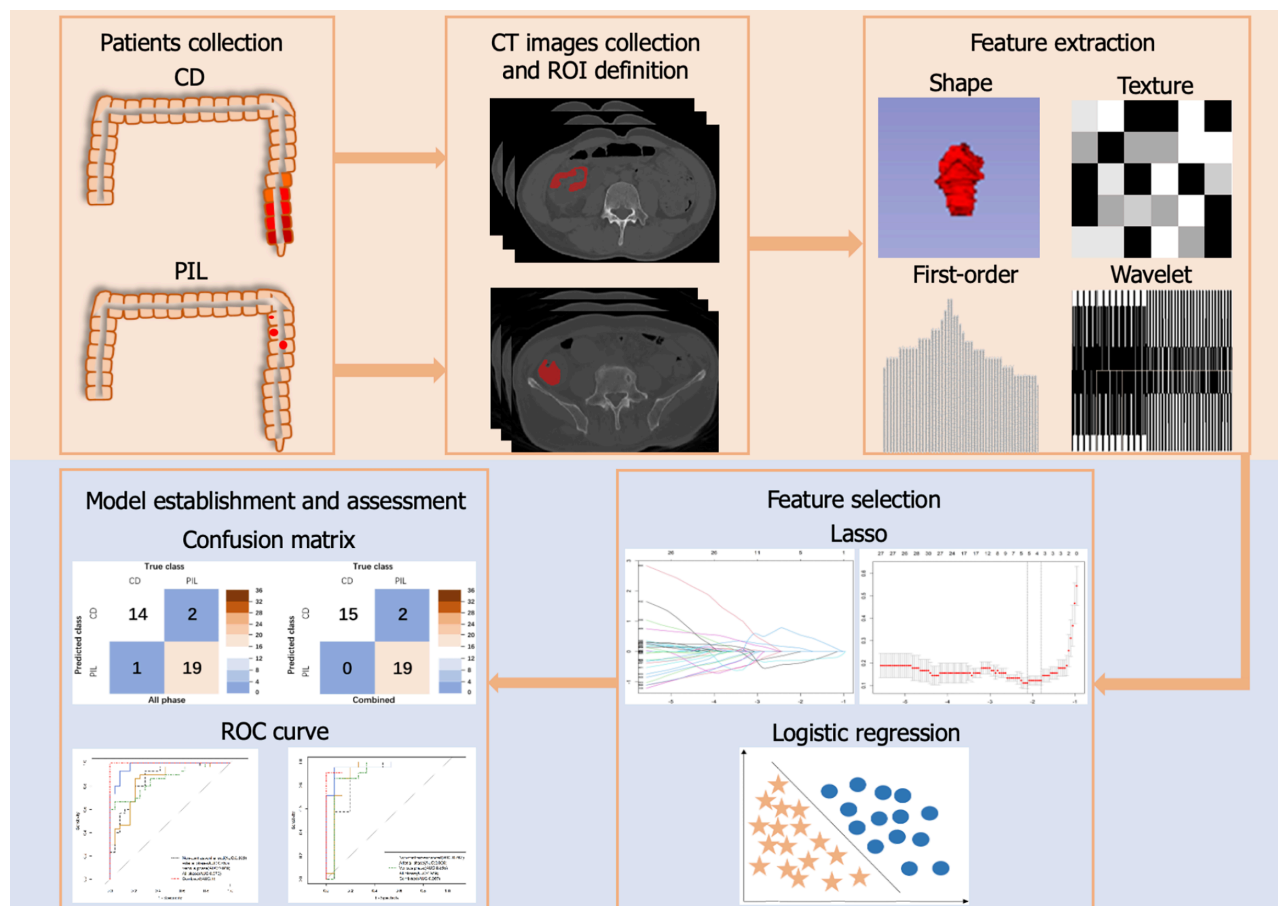


**Figure 1** Flowchart of radiomics and clinical-radiomics model construction to classify primary intestinal lymphoma and Crohn's disease. CD: Crohn's disease; PIL: Primary intestinal lymphoma; CT: Computed tomography; ROI: Region of interest; ROC: Receive operating curve; Lasso: Least absolute shrinkage and selection operator.

In this study, we combined clinical factors and radiomic features to develop an all phase model based on three-phase CT and a combined model based on clinical features and three-phase CT, respectively. Among them, the model combining clinical data and radiological features has the highest performance, and the AUC value of this model exceeds 0.980 in the training set, internal validation set and external validation set. The combined model has good discriminatory value for the diagnosis of PIL and CD and plays an important role in assisting doctors in choosing the appropriate treatment plan.

CT is considered the most common and valuable tool for the evaluation of intestinal diseases, especially contrast-enhanced computed tomography (CECT), which allows diagnosis and differentiation of intestinal diseases by multiphase scanning[4]. However, in clinical work, PIL and CD share some similar imaging features, such as bowel-wall thickening,

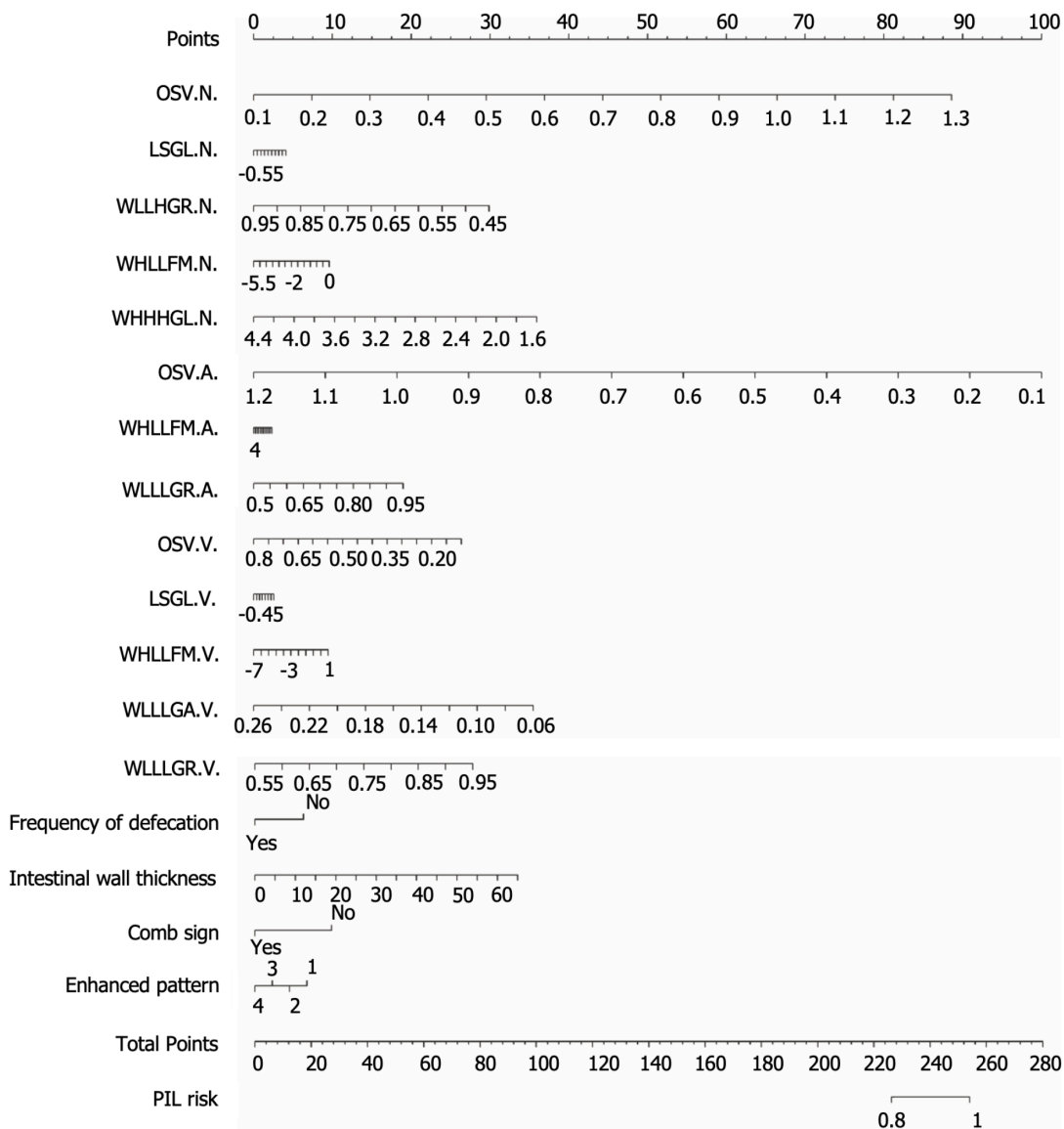


**Figure 2 The nomogram of combined model.** Gender: 1-Male; 2-Female; Enhanced pattern: 1-Homogeneous enhancement; 2-Inhomogeneous enhancement; 3-Hierarchical enhancement; 4-Mucosal enhancement. PIL: Primary intestinal lymphoma; OSV: Original shape voxel volume; LSGL: Log sigma 3-0-mm-3D glcm lmc2; WLLHGR: Wavelet LLH glrlm run percentage; WHLLFM: Wavelet HLL firstorder minimum; WHHHGL: Wavelet HHH glrlm long run high gray level emphasis; WLLGR: Wavelet LLL glrlm run percentage; WLLGA: Wavelet LLL glcm autocorrelation; N: Non-contrast enhanced; A: Arterial; V: Venous.

enlargement of regional lymph nodes, and enhancement of the lesion after enhanced scan[7]. In general, substantial thickening of the intestinal wall (approximately 2 cm), aneurysmal dilatation, and uniform enhancement contribute to the diagnosis of PIL. In CD, mild intestinal wall thickening, layered strengthening of the intestinal wall and multi-segmental involvement of the intestine are more common[2]. However, some pathological types of PIL, such as enteropathy-associated T-cell lymphoma, may have a pattern of enhancement that is very similar to CD, showing stratified enhancement. Similarly, CD sometimes shows homogeneous enhancement of the intestinal wall on enhancement scans that is indistinguishable from PIL[23]. In addition, although endoscopic biopsy is the gold standard for the diagnosis of lymphoma, it is difficult to accurately obtain tumor tissue under endoscopy in clinical work when the lesion is small in size or the tumor site is deep[6,7]. In this study, there were some patients with PIL diagnosed with CD at first due to the results of the initial tissue biopsy under endoscopy. However, after repeated pathological biopsies under endoscopy, the final diagnosis was PIL. Therefore, we believe that the combination of clinical data, noninvasive imaging examinations and artificial intelligence is more conducive to the differential diagnosis of diseases.

In clinical practice, reliable identification of PIL and CD is critical to the choice of patient treatment options. Previous studies have focused solely on the evaluation of morphological manifestations and imaging features of intestinal disease, including clinically relevant data, endoscopic features, and imaging signs[7,24]. In terms of radiomics, we were unable retrieve information from the literature on the differentiation of PIL and CD by imaging histology combined with machine learning, probably due to the rarity of these two diseases. However, some studies have applied CT texture parameters to differentiate intrahepatic cholangiocarcinoma from hepatic lymphoma[25]. Inspired by the above studies, we combined clinical data with radiomic analysis of CT images to construct a more refined discriminatory model.

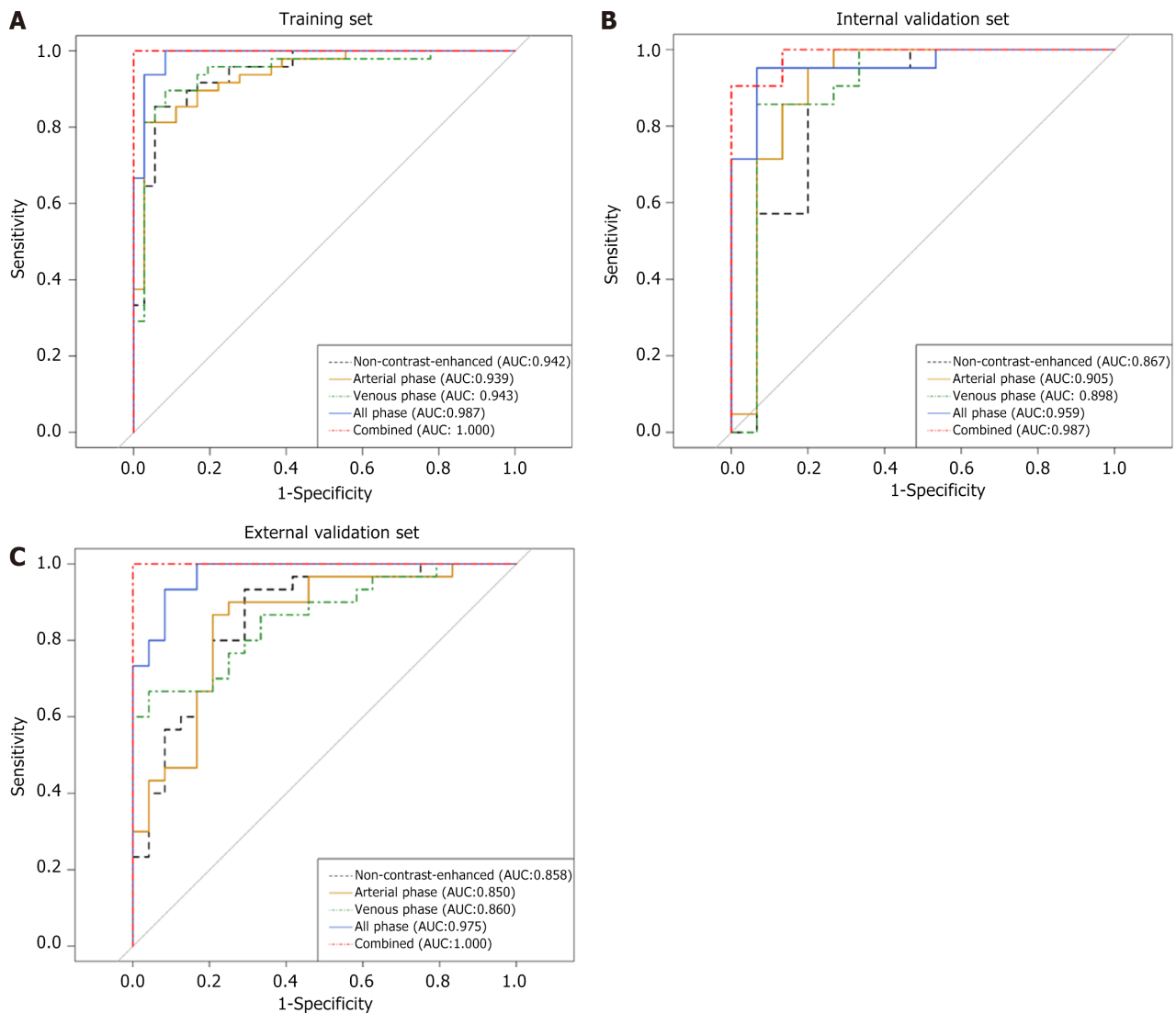


**Figure 3** The receive operating curves. A: The receive operating curves of models based on the training set; B: The receive operating curves of models based on the internal validation set; C: The receive operating curves of models based on the external validation set. AUC: Area under the curve.

In previous studies, Zhang *et al*[7] retrospectively collected data on patients with CD and PIL, including clinical information and imaging features. After the analysis, a classification model with high specificity was established, with an accuracy, a specificity and a sensitivity of 0.936, 0.964 and 0.918, respectively. In contrast, our study collected clinical data and laboratory indices, but also collected multi-phase CT images including non-contrast enhanced phase, arterial phase and venous phase, and further extracted radiomic features of the images. Liu *et al*[4] performed preoperative differential diagnosis of lymphoma and other small intestinal malignancies by CT texture analysis, and established the clinical model, arterial texture model and venous texture model by outlining the ROI at the maximum level to extract features, respectively, and their AUCs all reached above 0.87. Differently, our study is dedicated to the identification of PIL and CD, rather than simply classifying patients with disease into lymphoma and non-lymphoma groups to achieve a clearer clinical localization. In addition, we extracted radiomic features based on shape, first-order and texture features by multi-level 3D segmentation on three-phase CT images and combined them with characteristic clinical factors to build a combined model with higher classification power (AUC = 1.000). Our study performed richer feature extraction and obtained higher AUC models. The combined model has a higher AUC of 1.000 compared to the simple all-time phase model. Recently, Yang *et al*[24] developed a scoring model to discriminate PIL from CD based on clinical symptoms, endoscopic and imaging features, with an accuracy of 83.66% and an AUC of 0.947. In addition, they further evaluated the performance of the model by tenfold cross-validation (AUC = 0.901). The difference is that, on the one hand, we used a simple and readable nomogram and, on the other hand, we add an external validation set from another center, which allows for a more comprehensive evaluation of the mode. Among them, the combined model shows the best performance, with a higher AUC on the external validation set than on the internal validation set, with an AUC of 1.000. Compared to the models built in previous studies, our model shows a more outstanding discrimination on the external validation set, with an accuracy, specificity and sensitivity of 1.000.

PIL and CD have completely different treatment modalities. The treatment of CD is aimed at induction followed by maintenance of remission. Immunosuppressive agents and 5-aminosalicylic acid analogs are used as the main therapeutic

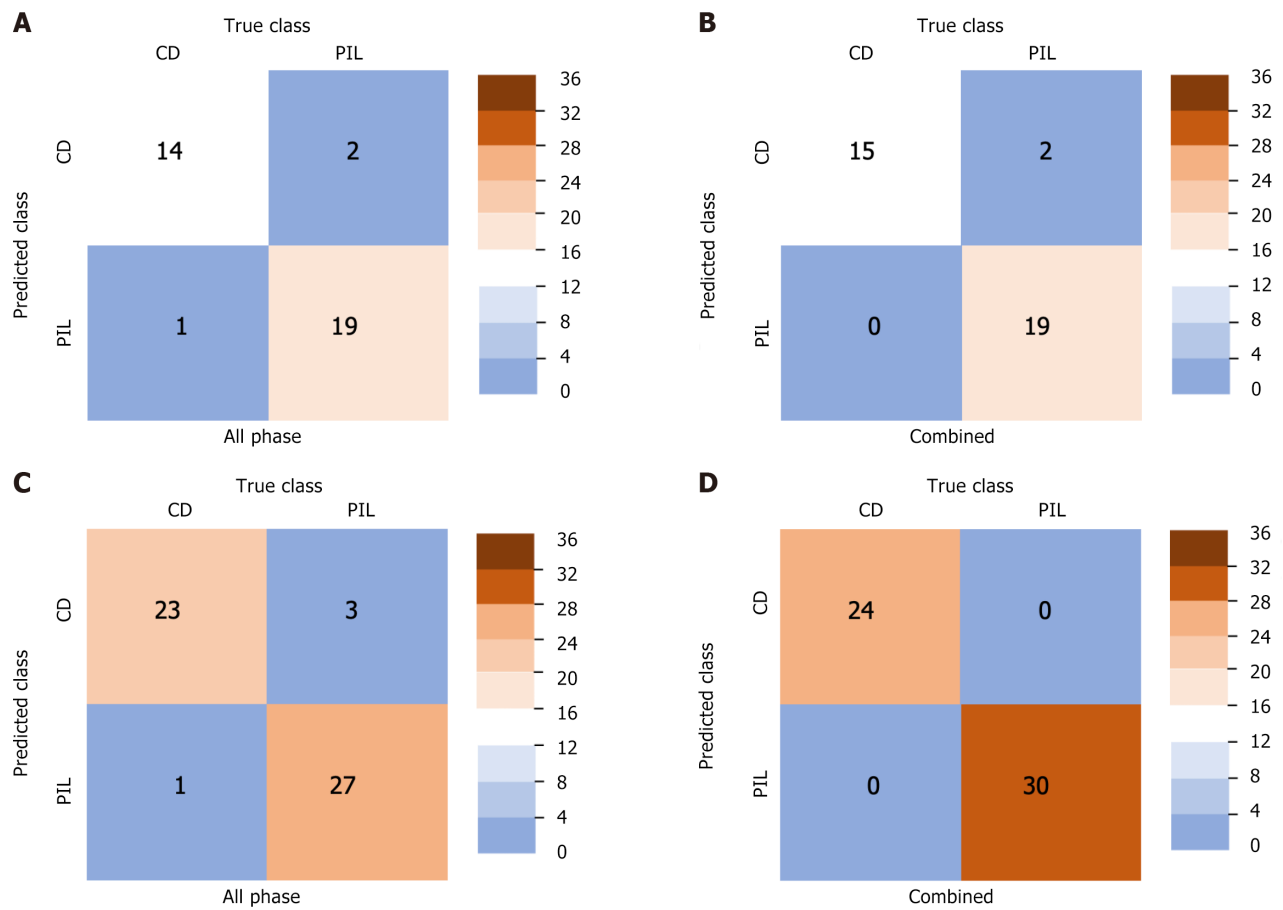


**Figure 4 The confusion matrix.** A: The performance of all phase radiomics model in the internal validation set; B: The performance of combined model in the internal validation set; C: The performance of all phase radiomics model in the external validation set; D: The performance of combined model in the external validation set. CD: Crohn's disease; PIL: Primary intestinal lymphoma.

agents for the treatment of moderate-to-severe and mild-to-moderate CD, respectively. If the disease continues to progress, biological therapies may be used for disease induction and control[10,26]. Treatment of PIL is diverse, ranging from simple "wait and see" to local radiotherapy or surgery to chemotherapy and stem cell transplantation. Most studies support an approach based on the World Health Organization classification and the Ann Arbor or Paris staging system to determine diagnosis and staging, followed by individualized treatment in conjunction with the patient's own condition [27,28]. Some studies claim that delayed diagnosis may affect the disease process, often leading to complications, such as stenosis and endovascular fistulae in CD, which prevent remission[29,30]. A study of adult CD patients in France showed that delaying diagnosis for more than 13 months is associated with a high risk of major surgery[29]. Therefore, early, rapid and accurate disease diagnosis is crucial to the treatment and prognosis of PIL and CD and is a great challenge for clinicians.

Our study has some limitations. First, this study was retrospective, and diseases other than PIL and CD were not included in the analysis. Therefore, clinicians would need to exclude other diseases before attempting to differentiate the two diseases, which may limit the use of the model in clinical practice. Second, because this study was retrospective, the images were obtained from different CT machine scans, which may cause discrepancies between the original images. In addition, the case data in this study were limited because PIL and CD are relatively rare. A larger amount of data would allow the model to achieve a more robust assessment, and its performance may improve. Finally, we will further improve the technical level and increase the amount of clinical data in anticipation of applying deep learning to the differential diagnosis of PIL and CD. The above will be the focus of our further study.

## CONCLUSION

In conclusion, we report that CECT-based radiomics combined with machine learning models can be used to differentiate PIL from CD on images. The developed model has the ability to provide a valuable reference for clinicians in rapid diagnosis and determination of treatment options.

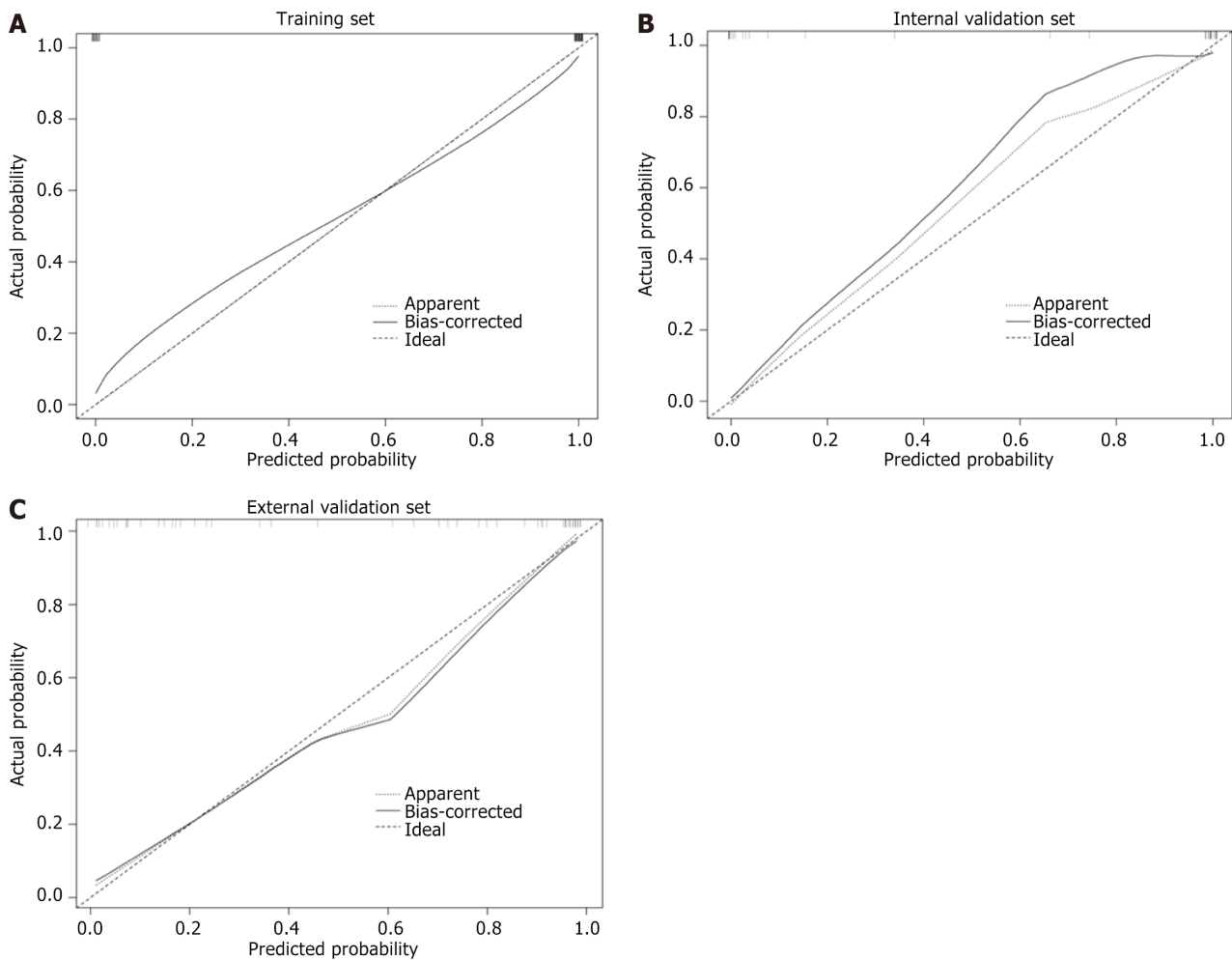


**Figure 5 The calibration curve.** A: The calibration curve of combined model in the training set; B: The calibration curve of combined model in the internal validation set; C: The calibration curve of combined model in the external validation set.

## ACKNOWLEDGEMENTS

We would like to express our special thanks of gratitude to Dr. Hua Fan for her statistical advice. We thank all authors for their contributions to the conceptualization and design of the study.

## FOOTNOTES

**Author contributions:** Xiao MJ and Pan YT have the equal contribution to the manuscript; Xiao MJ, Pan YT, and Wang HY contributed to the conception and design of the research, they also contributed to the revision of manuscript for important intellectual content; Xiao MJ, Pan YT and Li HO contributed to the acquisition of data; Xiao MJ and Pan YT contributed to the analysis and interpretation of data and contributed to the drafting the manuscript; Wang HY contributed to the obtaining funding; All authors have read and approve the final manuscript.

**Supported by** Key Technology Research and Development Program of Shandong Province, China, No. 2021SFGC0104.

**Institutional review board statement:** This study was reviewed and approved by the Ethics Committee of Shandong Provincial Hospital Affiliated to Shandong First Medical University, China, NO. 2023-422.

**Informed consent statement:** Informed consent has been obtained for the publication of experimental data and images.

**Conflict-of-interest statement:** We have no financial relationships to disclose.

**Data sharing statement:** No additional data are available.

**Open-Access:** This article is an open-access article that was selected by an in-house editor and fully peer-reviewed by external reviewers. It is distributed in accordance with the Creative Commons Attribution NonCommercial (CC BY-NC 4.0) license, which permits others to distribute, remix, adapt, build upon this work non-commercially, and license their derivative works on different terms, provided the

original work is properly cited and the use is non-commercial. See: <https://creativecommons.org/licenses/by-nc/4.0/>

**Country of origin:** China

**ORCID number:** Hai-Yan Wang [0000-0002-8506-7604](https://orcid.org/0000-0002-8506-7604).

**S-Editor:** Fan M

**L-Editor:** A

**P-Editor:** Zhang XD

## REFERENCES

- 1 **Arora N**, Manipadam MT, Pulimood A, Ramakrishna BS, Chacko A, Kurian SS, Nair S. Gastrointestinal lymphomas: pattern of distribution and histological subtypes: 10 years experience in a tertiary centre in South India. *Indian J Pathol Microbiol* 2011; **54**: 712-719 [PMID: [22234096](https://pubmed.ncbi.nlm.nih.gov/22234096/) DOI: [10.4103/0377-4929.91502](https://doi.org/10.4103/0377-4929.91502)]
- 2 **Kumar P**, Singh A, Deshmukh A, Chandrashekhara SH. Imaging of Bowel Lymphoma: A Pictorial Review. *Dig Dis Sci* 2022; **67**: 1187-1199 [PMID: [33877497](https://pubmed.ncbi.nlm.nih.gov/33877497/) DOI: [10.1007/s10620-021-06979-3](https://doi.org/10.1007/s10620-021-06979-3)]
- 3 **Gustafsson BI**, Siddique L, Chan A, Dong M, Drozdov I, Kidd M, Modlin IM. Uncommon cancers of the small intestine, appendix and colon: an analysis of SEER 1973-2004, and current diagnosis and therapy. *Int J Oncol* 2008; **33**: 1121-1131 [PMID: [19020744](https://pubmed.ncbi.nlm.nih.gov/19020744/)]
- 4 **Liu S**, Zhang C, Liu R, Li S, Xu F, Liu X, Li Z, Hu Y, Ge Y, Chen J, Zhang Z. CT Texture Analysis for Preoperative Identification of Lymphoma from Other Types of Primary Small Bowel Malignancies. *Biomed Res Int* 2021; **2021**: 5519144 [PMID: [33884262](https://pubmed.ncbi.nlm.nih.gov/33884262/) DOI: [10.1155/2021/5519144](https://doi.org/10.1155/2021/5519144)]
- 5 **Ghimire P**, Wu GY, Zhu L. Primary gastrointestinal lymphoma. *World J Gastroenterol* 2011; **17**: 697-707 [PMID: [21390139](https://pubmed.ncbi.nlm.nih.gov/21390139/) DOI: [10.3748/wjg.v17.i6.697](https://doi.org/10.3748/wjg.v17.i6.697)]
- 6 **Nakamura S**, Matsumoto T. Gastrointestinal lymphoma: recent advances in diagnosis and treatment. *Digestion* 2013; **87**: 182-188 [PMID: [23635497](https://pubmed.ncbi.nlm.nih.gov/23635497/) DOI: [10.1159/000350051](https://doi.org/10.1159/000350051)]
- 7 **Zhang TY**, Lin Y, Fan R, Hu SR, Cheng MM, Zhang MC, Hong LW, Zhou XL, Wang ZT, Zhong J. Potential model for differential diagnosis between Crohn's disease and primary intestinal lymphoma. *World J Gastroenterol* 2016; **22**: 9411-9418 [PMID: [27895429](https://pubmed.ncbi.nlm.nih.gov/27895429/) DOI: [10.3748/wjg.v22.i42.9411](https://doi.org/10.3748/wjg.v22.i42.9411)]
- 8 **Panneerselvam K**, Goyal S, Shirwaikar Thomas A. Ileo-colonic lymphoma: presentation, diagnosis, and management. *Curr Opin Gastroenterol* 2021; **37**: 52-58 [PMID: [33105251](https://pubmed.ncbi.nlm.nih.gov/33105251/) DOI: [10.1097/MOG.0000000000000687](https://doi.org/10.1097/MOG.0000000000000687)]
- 9 **Torres J**, Mehndru S, Colombel JF, Peyrin-Biroulet L. Crohn's disease. *Lancet* 2017; **389**: 1741-1755 [PMID: [27914655](https://pubmed.ncbi.nlm.nih.gov/27914655/) DOI: [10.1016/S0140-6736\(16\)31711-1](https://doi.org/10.1016/S0140-6736(16)31711-1)]
- 10 **Lichtenstein GR**, Loftus EV, Isaacs KL, Regueiro MD, Gerson LB, Sands BE. ACG Clinical Guideline: Management of Crohn's Disease in Adults. *Am J Gastroenterol* 2018; **113**: 481-517 [PMID: [29610508](https://pubmed.ncbi.nlm.nih.gov/29610508/) DOI: [10.1038/ajg.2018.27](https://doi.org/10.1038/ajg.2018.27)]
- 11 **Liu YY**, Chen MK, Cao Z, Liu SZ, Ding BJ. Differential diagnosis of intestinal tuberculosis from Crohn's disease and primary intestinal lymphoma in China. *Saudi J Gastroenterol* 2014; **20**: 241-247 [PMID: [25038210](https://pubmed.ncbi.nlm.nih.gov/25038210/) DOI: [10.4103/1319-3767.136979](https://doi.org/10.4103/1319-3767.136979)]
- 12 **Zalis M**, Singh AK. Imaging of inflammatory bowel disease: CT and MR. *Dig Dis* 2004; **22**: 56-62 [PMID: [15292695](https://pubmed.ncbi.nlm.nih.gov/15292695/) DOI: [10.1159/000078735](https://doi.org/10.1159/000078735)]
- 13 **Kilcoyne A**, Kaplan JL, Gee MS. Inflammatory bowel disease imaging: Current practice and future directions. *World J Gastroenterol* 2016; **22**: 917-932 [PMID: [26811637](https://pubmed.ncbi.nlm.nih.gov/26811637/) DOI: [10.3748/wjg.v22.i3.917](https://doi.org/10.3748/wjg.v22.i3.917)]
- 14 **Panizza PS**, Viana PC, Horvat N, Dos Santos VR Júnior, de Araújo DA, Yamanari TR, Leite CD, Cerri GG. Inflammatory Bowel Disease: Current Role of Imaging in Diagnosis and Detection of Complications: Gastrointestinal Imaging. *Radiographics* 2017; **37**: 701-702 [PMID: [28287943](https://pubmed.ncbi.nlm.nih.gov/28287943/) DOI: [10.1148/rg.2017160050](https://doi.org/10.1148/rg.2017160050)]
- 15 **Lambin P**, Leijenaar RTH, Deist TM, Peerlings J, de Jong EEC, van Timmeren J, Sanduleanu S, Larue RTHM, Even AJG, Jochems A, van Wijk Y, Woodruff H, van Soest J, Lustberg T, Roelofs E, van Elmpt W, Dekker A, Mottaghy FM, Wildberger JE, Walsh S. Radiomics: the bridge between medical imaging and personalized medicine. *Nat Rev Clin Oncol* 2017; **14**: 749-762 [PMID: [28975929](https://pubmed.ncbi.nlm.nih.gov/28975929/) DOI: [10.1038/nrclinonc.2017.141](https://doi.org/10.1038/nrclinonc.2017.141)]
- 16 **Mayerhoefer ME**, Materka A, Langs G, Häggström I, Szczypiński P, Gibbs P, Cook G. Introduction to Radiomics. *J Nucl Med* 2020; **61**: 488-495 [PMID: [32060219](https://pubmed.ncbi.nlm.nih.gov/32060219/) DOI: [10.2967/jnumed.118.222893](https://doi.org/10.2967/jnumed.118.222893)]
- 17 **Gillies RJ**, Kinahan PE, Hricak H. Radiomics: Images Are More than Pictures, They Are Data. *Radiology* 2016; **278**: 563-577 [PMID: [26579733](https://pubmed.ncbi.nlm.nih.gov/26579733/) DOI: [10.1148/radiol.2015151169](https://doi.org/10.1148/radiol.2015151169)]
- 18 **Lambin P**, Rios-Velazquez E, Leijenaar R, Carvalho S, van Stiphout RG, Granton P, Zegers CM, Gillies R, Boellard R, Dekker A, Aerts HJ. Radiomics: extracting more information from medical images using advanced feature analysis. *Eur J Cancer* 2012; **48**: 441-446 [PMID: [22257792](https://pubmed.ncbi.nlm.nih.gov/22257792/) DOI: [10.1016/j.ejca.2011.11.036](https://doi.org/10.1016/j.ejca.2011.11.036)]
- 19 **Deo RC**. Machine Learning in Medicine. *Circulation* 2015; **132**: 1920-1930 [PMID: [26572668](https://pubmed.ncbi.nlm.nih.gov/26572668/) DOI: [10.1161/CIRCULATIONAHA.115.001593](https://doi.org/10.1161/CIRCULATIONAHA.115.001593)]
- 20 **Jordan MI**, Mitchell TM. Machine learning: Trends, perspectives, and prospects. *Science* 2015; **349**: 255-260 [PMID: [26185243](https://pubmed.ncbi.nlm.nih.gov/26185243/) DOI: [10.1126/science.aaa8415](https://doi.org/10.1126/science.aaa8415)]
- 21 **Dawson IM**, Cornes JS, Morson BC. Primary malignant lymphoid tumours of the intestinal tract. Report of 37 cases with a study of factors influencing prognosis. *Br J Surg* 1961; **49**: 80-89 [PMID: [13884035](https://pubmed.ncbi.nlm.nih.gov/13884035/) DOI: [10.1002/bjs.18004921319](https://doi.org/10.1002/bjs.18004921319)]
- 22 **Yushkevich PA**, Piven J, Hazlett HC, Smith RG, Ho S, Gee JC, Gerig G. User-guided 3D active contour segmentation of anatomical structures: significantly improved efficiency and reliability. *Neuroimage* 2006; **31**: 1116-1128 [PMID: [16545965](https://pubmed.ncbi.nlm.nih.gov/16545965/) DOI: [10.1016/j.neuroimage.2006.01.015](https://doi.org/10.1016/j.neuroimage.2006.01.015)]
- 23 **Pesce Lamas Constantino C**, Souza Rodrigues R, Araujo Oliveira Neto J, Marchiori E, Eiras Araujo AL, Perez Rde M, Braz Parente D. Computed tomography and magnetic resonance enterography findings in Crohn's disease: what does the clinician need to know from the

- radiologist? *Can Assoc Radiol J* 2014; **65**: 42-51 [PMID: 23706867 DOI: 10.1016/j.carj.2012.11.004]
- 24 **Yang H**, Zhang H, Liu W, Tan B, Guo T, Gao X, Feng R, Wu K, Cao Q, Ran Z, Liu Z, Hu N, Zhu L, Lai Y, Wang C, Han W, Qian J. Differential Diagnosis of Crohn's Disease and Ulcerative Primary Intestinal Lymphoma: A Scoring Model Based on a Multicenter Study. *Front Oncol* 2022; **12**: 856345 [PMID: 35586498 DOI: 10.3389/fonc.2022.856345]
- 25 **Xu H**, Zou X, Zhao Y, Zhang T, Tang Y, Zheng A, Zhou X, Ma X. Differentiation of Intrahepatic Cholangiocarcinoma and Hepatic Lymphoma Based on Radiomics and Machine Learning in Contrast-Enhanced Computer Tomography. *Technol Cancer Res Treat* 2021; **20**: 15330338211039125 [PMID: 34499018 DOI: 10.1177/15330338211039125]
- 26 **Wright EK**, Ding NS, Niewiadomski O. Management of inflammatory bowel disease. *Med J Aust* 2018; **209**: 318-323 [PMID: 30257634 DOI: 10.5694/mja17.01001]
- 27 **Beaton C**, Davies M, Beynon J. The management of primary small bowel and colon lymphoma--a review. *Int J Colorectal Dis* 2012; **27**: 555-563 [PMID: 21912877 DOI: 10.1007/s00384-011-1309-2]
- 28 **Cardona DM**, Layne A, Lagoo AS. Lymphomas of the gastro-intestinal tract - pathophysiology, pathology, and differential diagnosis. *Indian J Pathol Microbiol* 2012; **55**: 1-16 [PMID: 22499293 DOI: 10.4103/0377-4929.94847]
- 29 **Agrawal M**, Spencer EA, Colombel JF, Ungaro RC. Approach to the Management of Recently Diagnosed Inflammatory Bowel Disease Patients: A User's Guide for Adult and Pediatric Gastroenterologists. *Gastroenterology* 2021; **161**: 47-65 [PMID: 33940007 DOI: 10.1053/j.gastro.2021.04.063]
- 30 **Stankovic B**, Kotur N, Nikcevic G, Gasic V, Zukic B, Pavlovic S. Machine Learning Modeling from Omics Data as Prospective Tool for Improvement of Inflammatory Bowel Disease Diagnosis and Clinical Classifications. *Genes (Basel)* 2021; **12** [PMID: 34573420 DOI: 10.3390/genes12091438]



Published by **Baishideng Publishing Group Inc**  
7041 Koll Center Parkway, Suite 160, Pleasanton, CA 94566, USA  
**Telephone:** +1-925-3991568  
**E-mail:** [office@baishideng.com](mailto:office@baishideng.com)  
**Help Desk:** <https://www.f6publishing.com/helpdesk>  
<https://www.wjgnet.com>

